Accepted Manuscript

Terminal functionalized thiourea-containing dipeptides as multidrug-resistance reversers that target 20S proteasome and cell proliferation

Jian-Mei Qin, Ri-Zheng Huang, Gui-Yang Yao, Zhi-Xin Liao, Ying-Ming Pan, Heng-Shan Wang

PII: S0223-5234(16)30962-X

DOI: 10.1016/j.ejmech.2016.11.024

Reference: EJMECH 9057

To appear in: *European Journal of Medicinal Chemistry*

Received Date: 13 September 2016

Revised Date: 7 November 2016

Accepted Date: 10 November 2016

Please cite this article as: J.-M. Qin, R.-Z. Huang, G.-Y. Yao, Z.-X. Liao, Y.-M. Pan, H.-S. Wang, Terminal functionalized thiourea-containing dipeptides as multidrug-resistance reversers that target 20S proteasome and cell proliferation, *European Journal of Medicinal Chemistry* (2016), doi: 10.1016/j.ejmech.2016.11.024.

Graphical abstract

Terminal functionalized thiourea-containing dipeptides as multidrug-resistance reversers that target 20S proteasome and cell proliferation

Jian-Mei Qin, Ri-Zheng Huang, Gui-Yang Yao, Zhi-Xin Liao, Ying-Ming Pan and Heng-Shan Wang

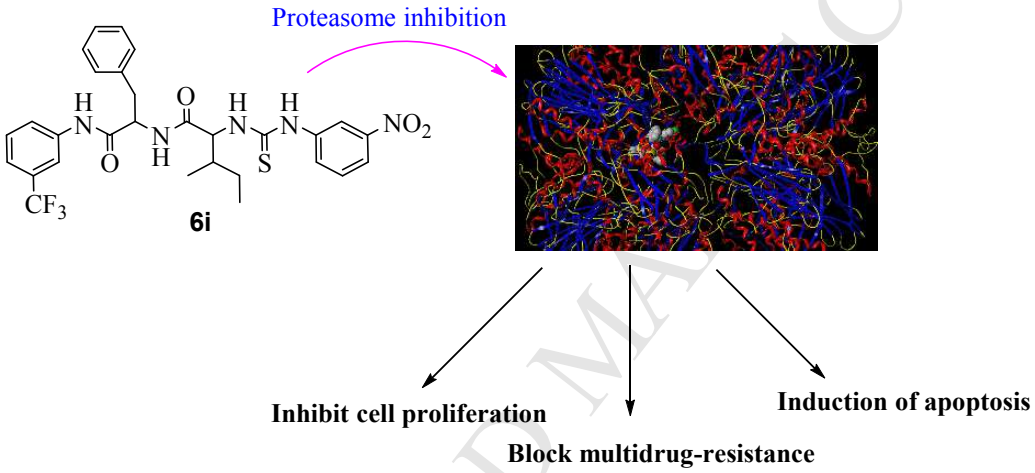

Terminal functionalized thiourea-containing dipeptides as multidrug-resistance reversers that target 20S proteasome and cell proliferation

Jian-Mei Qin[a, †], Ri-Zheng Huang[b, †], Gui-Yang Yao[b], Zhi-Xin Liao[b], Ying-Ming Pan[a *] and Heng-Shan Wang[a*]

[a] *State Key Laboratory for the Chemistry and Molecular Engineering of Medicinal Resources (Ministry of Education of China), School of Chemistry and Pharmaceutical Sciences of Guangxi Normal University, Guilin 541004, PR China*

[b] *Pharmaceutical Research Center and School of Chemistry and Chemical Engineering, Southeast University, Nanjing 211189, China*

* Corresponding author.

*Corresponding author. E-mail addresses: whengshan@163.com (H. -S. Wang), panym2013@hotmail.com (Y.-M. Pan).

[†] Co-first author: These authors contributed equally to this work.

Abstract

A series of inhibitors of 20S proteasome based on terminal functionalized dipeptide derivatives containing the thiourea moiety were synthesized and evaluated for inhibition of 20S proteasome and the effects of multidrug-resistance reversers. These compounds exhibited significant selectivity to the β5-subunit of the human 20S proteasome with IC_{50} values at submicromolar concentrations. A docking study of the most active compound **6i** revealed key interactions between **6i** and the active site of the 20S proteasome in which the thiourea moiety and a nitro group were important for improving activity. In particular, compound **6i** appeared to be the most potent compound against the NCI-H460 cell line, and displayed similar efficiency in drug-sensitive versus drug-resistant cancer cell lines, at least partly, by inhibition of the activity of 20S proteasome and induce apoptosis. In addition, **6i**-induced apoptosis was significantly facilitated in NCI-H460/DOX cells that had been pretreated with inhibitors of P-gp. Mechanistically, compound **6i** might trigger apoptotic signalling pathway. Thus, we conclude that dipeptide derivatives containing the thiourea moiety may be the potential inhibitors of proteasome with the ability to reverse multidrug resistance.

keywords: Pseudopeptides; Thioureas; Proteasome; Anti-tumor; Multidrug resistance

1. Introduction

Multidrug resistance (MDR), the principal mechanism by which many cancers develop resistance to a variety of chemotherapeutic drugs, is a major impediment to effective cancer treatment with conventional chemotherapeutic drugs and has been intensively studied for the past three decades. The molecular mechanisms of MDR are complex and include extrusion of the drug by cell membrane pumps, such as P-glycoprotein (P-gp) or multidrug resistance-associated protein (MRP), modification of drug target molecules, enhanced drug detoxification, suppression of drug-induced apoptosis, increased DNA damage repair, upregulation of lipids and other biochemical changes [1]. As clinical drug resistance frequently hinders the treatment of neoplastic disease, extensive research has been carried out, but to date, no useful method for reversing MDR suitable for clinical use has been developed, thus creating the need for new classes of potent and specific anticancer drugs.

The ubiquitin-proteasome system (UPS), responsible for regulating cellular protein homeostasis via enzymatic cascades, plays a crucial role in mediating many normal cellular processes, including the cell cycle, differentiation and apoptosis [2, 3]. The proteasome is a major site for degradation of abnormal or irrelevant and regulatory proteins, such as transcription factors, oncoproteins, cyclins and anti-apoptotic proteins, which might be responsible for various types of drug resistance [2]. The 20S proteasome, composed of three distinct proteolytically active sites, β5, β2 and β1, is responsible for chymotrypsin-like (ChT-L), trypsin-like (T-L), and post-glutamyl peptide hydrolyzing (PGPH) or caspase-like proteolytic activities, respectively, and is the main proteolytic component of this degradation system [4]. Given that the inhibition of proteasome results in a myriad of cell responses and perturbed pathways, proteasome inhibitors provide a solution for re-sensitizing tumor cells to chemotherapy or to delay the development of treatment resistance [5]. Several proteasome inhibitors are in clinical trials or have been approved by the FDA, such as bortezomib [6], carfilzomib [7] and ixazomib [8] (Fig. 1). Recent studies have demonstrated the effectiveness of bortezomib, which is the first Food and Drug Administration (FDA)-approved proteasome inhibitor, in the treatment of relapsed and/or refractory multiple myeloma [9] and mantle cell lymphoma [10]. Bortezomib induces apoptosis in many types of tumor cells through the formation of reactive oxygen species (ROS) and endoplasmic reticulum (ER) stress [11-13]. The mitochondrial release of cytochrome c, apoptosis-inducing factor, and

cleavage of caspases has been demonstrated in cells undergoing bortezomib-induced apoptosis [14, 15]. Moreover, the proteasome inhibitor, MG132, which effectively blocks the proteolytic activity of the 26S proteasome complex, has been identified as an inhibitor of NF-κB, and suppression of NF-κB activation causes downregulation of anti-apoptotic Bcl-2 and MDR1 (P-gp) expression [16-18]. However, both bortezomib and the other proteasome inhibitors under clinical evaluation are limited due to severe side effects, acquired drug resistance, peripheral neuropathy, hematological toxicity and unsatisfactory pharmacokinetic profiles.

Due to these limitations, the development of pseudopeptides could lead to many pharmacokinetic and pharmacodynamic advantages [19, 20]. This strategy can be realized by introducing unnatural amino acids instead of natural residues into the peptide framework, or by the introduction of a non-peptidic scaffold into the peptidic backbone, in order to lock a defined conformation of the peptide [21, 22]. These novel compounds provide new perspectives in drug design by providing an entire range of highly specific and non-toxic pharmaceuticals. In addition to increased stability, the incorporation of a thiourea moiety into the peptide sequence also provides access to additional binding interactions within the transition state conformation of the enzyme/substrate complex [23, 24]. Thiourea could strongly enhance blocking since sulfur is the weaker hydrogen bond acceptor as compared to the amide carbonyl oxygen, and simultaneously enhance hydrogen-bonding due to the bidentate binding mode of the more acidic thiourea protons [25, 26]. Some peptide scaffold based on thiourea or bis(thiourea) motif have been reported as inhibitors of β-sheet aggregation and antitumor agents in recent years [24, 27]. Herein, we designed and synthesized a series of dipeptide thiourea derivatives as multidrug-resistance reversers which target 20S proteasome. The covalent binding mode of the designed inhibitors was subsequently clarified by performing a docking analysis using the crystal structure of the yeast 20S proteasome. Moreover, growth inhibitory effects were evaluated against six human tumor cell lines and doxorubicin-resistant cell lines. The molecular mechanism of apoptosis in NCI-H460 cells by the representative target compound **6i** was also investigated.

2. Results and Discussion

2.1 Chemistry

The general procedures for the synthesis of functionalized dipeptide thioureas are shown in Scheme 1. First, Boc-amide and aniline derivatives underwent acylation and deprotection, and

each amino acid was sequentially coupled to the peptide chain from the C- to N-terminus in the presence of HOBt, EDCI and Et_3N. After obtaining the free amine dipeptide **5** by removal of the protective group, target compounds **6** was synthesized by the condensation of phenylisothiocyanate according to a previously published report [28] with **5** in DCM at room temperature. Dipeptide **7** was synthesized by alkylation of **6** with methyl iodide in the presence of K_2CO_3 according to a previously published study [29]. The structures of target compounds **6** and **7** were then confirmed by ^{1}H NMR, ^{13}C NMR and high resolution mass spectrometry (HRMS).

2.2 Biological evaluation

2.2.1 Inhibitory effect on the ChT-L, T-L and PGPH activities of human 20S proteasome

The inhibitory potency of all synthesized compounds was determined against the ChT-L activity of the human 20S proteasome as described previously [30], and MG132 was used as a reference compound. As shown in Table 1, most compounds showed significant inhibitory potency against ChT-L activity. Of these compounds, **6i**, **6k** and **6m** exhibited IC_{50} values at low micromolar or submicromolar levels. The preliminary structure-activity relationships of dipeptide thiourea derivatives for their ChT-L inhibitory activities are listed in Table 1. Analysis of the effects of the terminal substituents at the R^1 position of dipeptide thiourea derivatives showed that a fluorine or trifluoromethyl group generally enhanced ChT-L inhibition, compared with a methyl or methoxy group substitution. When the methoxy of compound **6a** was replaced with a fluorine group at the 3-position on the phenyl ring (compound **6d**), the inhibition potency was markedly increased, and the inhibitory activity was increased 4-fold compared with **6a**. Replacing the 4-position on the phenyl ring with a fluorine or bromine group at R^1 to yield compound **6g** and **6f**, respectively, resulted in a marked increase in potency, thus demonstrating that the electronic properties of the substituents may play a critical role in potent inhibitory activities against ChT-L. However, the introduction of two methyl groups hindered the inhibitory activity. Moreover, analogs with a methyl fragment at R^1 were much less active or completely inactive. A variation at R^1 could cause a substantial difference in inhibitory potency, presumably due to different affinity to the binding pocket. With regard to the effects of the electronic properties at R^2, the ChT-L inhibitory activities increased in the following order: bromine< trifluoromethyl < nitro. In particular, the most potent ChT-L inhibitor, **6i**, had an IC_{50} value against ChT-L of approximately 8.6 nM, thus illustrating that the nitro group was the optimal R^2 moiety. Substitution of the

thiourea group with methylated products markedly reduced ChT-L inhibitory activities, with the exception of compound **7b**, which may due to the positive contribution of the thiourea group to enzyme inhibition.

Four compounds, **6i**, **6k**, **6m** and **7b**, with the most potent inhibitory activity against ChT-L activity were further evaluated against the β1- and β2-subunits. All these compounds inhibited PGPH activity to a lesser extent than ChT-L activity, whereas no inhibition was observed against T-L activity. These results are particularly significant as the literature indicates that co-inhibition of ChT-L activity together with either PGPH or T-L activity could provide optimal anticancer agents [31], whereas inhibition of ChT-L activity alone produces only moderate effects [32], while the cytotoxicity of inhibitors correlates with inhibition of all activities [33]. These results suggest that this novel series of proteasome inhibitors could be selective for the β5-subunit of the 20S proteasome, which is consistent with previous observations on linear peptide proteasome inhibitors.

2.2.2 Molecular docking

To understand the interactions between the most active compound **6i** and the target of interest (20S proteasome), we performed molecular docking calculations on the active site of 20S proteasome (Fig. 2) using SYBYL-X 2.0 software and the results are summarized in Table 2. The interacting mode of compound **6i** (docking score 12.63), with the best docking score and interaction in the binding site of the 20S proteasome receptor, is described and compared with other derivatives and is shown in Figure 2. Some key residues, such as ILE24, GLY92, GLY98 and ASP116, as well as hydrogen bonds between the selected compound and the residues are also labeled. As shown in Figure 2a, compound **6i** was stabilized predominantly by the hydrophilic or hydrophobic group of ILE24, GLY92, GLY94 and ASP116. The nitro nitrogen and oxygen of the compound, which are the primary important moieties, formed a hydrogen-bond interaction network with the amino-acid residues GLY92, GLY94 and HOH of the active site. In addition, the polar hydrogen of the thiourea moiety formed three hydrogen bonds with the backbone carbonyl of SER115 and ASP116, which confirmed that this moiety is also crucial for binding. Furthermore, the trifluoromethyl group in the R^1 position as an acceptor established one hydrogen bond with ILE24. As expected, the dipeptide backbone formed a hydrogen bond with the active site residue (GLY128). In addition, the side chains of compound **6i** were closely integrated with residues

GLY47 and ASP114 of the active site. Specifically, the crucial electrostatic interactions between compound **6i** and residues ILE24, GLY92, ASP116 and GLY128 of 20S proteasome were observed in the binding pocket. Figure 2b shows that the interacting mode of 3E47-ligand in the binding site, which is a crucial electrostatic interaction between the ligand and residue GLY47, was observed in the binding pocket. The binding mode of the positive control MG132 in the ChT-L binding pocket is shown in Figure 2c. Hydrogen bonds with THR21, GLY47 and SER129 of the proteasome were observed in the docked structure.

2.2.3 Cytotoxicity Measurement

The in vitro antiproliferative activity of the dipeptide thiourea derivatives was evaluated by MTT assay in two parental cell lines (NCI-H460 and HepG2) and the corresponding DOX resistant cell lines (NCI-H460/DOX and HepG2/DOX), with doxorubicin (DOX) as the positive control. The results are shown in Table 3.

As shown in Table 3, most of the test compounds exhibited high inhibitory activity against the parental and resistant tumor cell lines, indicating that the introduction of thiourea and a nitro moiety on the dipeptide markedly increased anti-tumor activity. Moreover, the antiproliferative activities of the tested compounds correlated well with their ability to inhibit 20S proteasome, with activities depending on the substituents at the R^1 position, and followed the order $-NO_2$> $-CF_3$ > -Cl > -Br. Most of these compounds possessed either trifluoromethyl or polymethoxy moieties which may have had certain steric electronic properties which enhanced lipophilicity and the ability to penetrate the cellular membrane leading to an increased antiproliferative effect. In this regard, compound **6i** with a nitro moiety at R^2 and a trifluoromethyl moiety at R^1 was the best compound, depending on the cell line tested, with IC_{50} values of 1.70±1.16, 4.48±1.23, 6.74±1.87 and 10.18±1.53 μM against NCI-H460, HepG2, NCI-H460/DOX and HepG2/DOX cells, respectively, and thus was more potent and effective than doxorubicin.

As the selectivity of antitumor agents for cancer cells over non-malignant cells is important to avoid numerous severe side effects, all compounds were tested using a non-cancerous liver cell line (HL-7702). As shown in Table 3, the cytotoxicity activities of most compounds against cancer cells was much higher than that against HL-7702 normal cells, making them good candidates as anticancer drugs. In summary, these modifications yielded a small increase in cytotoxicity

activities compaired with doxorubicin and a low, but significant improvement in selectivity of the compounds.

*2.2.4 Compound **6i** induces apoptosis in NCI-H460 and NCI-H460/DOX cells*

In order to confirm whether **6i**-induced reduction in cell viability was responsible for the induction of apoptosis, NCI-H460 and NCI-H460/DOX cells were co-stained with 7-AAD and Annexin V-PE, and the number of apoptotic cells was estimated by flow cytometry (Fig. 3). Four quadrant images were observed by flow cytometric analysis: the Q1 area represented damaged cells which appearedduring the process of cell collection, the Q2 region showed necrotic cells and later stage apoptotic cells; early apoptotic cells were located in the Q3 area and the Q4 area showed normal cells. As shown in Figures 3, few (7.06%) apoptotic cells were present in the control panel, in contrast, the percentage rose to 21.06% at the concentration of 4 μM after treatment with **6i** for 24 h against NCI-H460 cells. Compound **6i** also remarkably induced NCI-H460/DOX cells apoptosis, with 17.36% apoptotic cells as compared with control (4.27). Interestingly, treatment of the cells with the specific P-gp inhibitor LY335979 had no significant effects on the parental cell lines but abolished MDR in the DOX-resistent NCI-H460/DOX cell lines, resulting in the apoptotic cells increase from 29.06 to 61.8%. This restored efficiency of this compound in the presence of the specific P-gp inhibitor illustrating that the resistance can be attributed to P-gp. Simultaneously, these results clearly confirmed that compared with the control, compound **6i** effectively induced apoptosis in NCI-H460 and NCI-H460/DOX cells.

3. Conclusions

A series of dipeptide thiourea derivatives were designed and synthesized as multidrug-resistance reversers which targeted 20S proteasome with high selectivity and an optimal inhibition profile. These compounds exhibited significant selectivity toward the β5-subunit of the human 20S proteasome with IC_{50} values at submicromolar concentrations. A docking study of the most active compound **6i** revealed key interactions between **6i** and the β5-subunit of the 20S proteasome in which the thiourea moiety and a nitro group were important for improving activity. It is noteworthy that further antitumor activity screening revealed that some compounds exhibited better inhibitory activity than the commercial anticancer drug doxorubicin, and selected compounds markedly reversed multidrug-resistance in DOX-resistant cancer cells. In particular, compound **6i** (IC_{50} = 1.70 ± 1.16 μM) exhibited the best anticancer activity against the NCI-H460

cell line and displayed more potent inhibitory activity than doxorubicin. Nevertheless, **6k** had a smaller resistance factor than **6i** and **6m**. The apoptosis-inducing activity investigated by flow cytometry revealed that compound **6i** markedly induced NCI-H460 and NCI-H460/DOX cells apoptosis. In addition, **6i**-induced apoptosis was significantly facilitated in NCI-H460/DOX cells that had been pretreated with inhibitors of P-gp. Consequently, the rational design of dipeptide thiourea derivatives offers significant potential for the discovery of a new class of proteasome inhibitors with the ability to reverse multidrug resistance. The precise mechanism of this action requires further investigation.

4. Experimental

4.1 General information

The isothiocyanate was synthesized according to the literature [23]. Compounds **5** were synthesized according to the literature [34]. All the chemical reagents and solvents used were of analytical grade. All amino acids were coupled as their N^a-Boc-derivatives. Silica gel (300-400 mesh) used in column chromatography was provided by Tsingtao Marine Chemistry Co. Ltd. Precoated silica gel plates F-254 were used for thin-layer analytical chromatography. ^{1}H-NMR and ^{13}C-NMR spectra were recorded on a Bruker AV-400spectrometer. High-resolution mass spectra (HRMS) were recorded on a Thermo-Scientific Exactive spectrometerusing ESI and APCI ionization sources.

4.2 General procedure for the preparation of isothiocyanate

Toluene (20 mL) was added to the amine (10 mmol) and TEDA (30.3mmol). CS_2 (30.3 mmol) were added while stirring, resulting in the precipitation of the dithiocarbamate. The reaction mixture was stirred for 8 h at room temperature and then filtered and dried. The resulting powder was suspended in the CH_2Cl_2 (20 mL), and cooled to 0°C and then triphosgene (BTC) (3.3mmol) was added. After complete the reaction at room temperature for 1h, and keep refluxing for 2 h. Insolubles were removed by filtration, and the solvent was purified by chromatography on silica gel eluted with petroleum ether to offer isothiocyanate.

4.3 General procedure for the preparation of peptides

*4.3.1 General procedure for compounds **2** and **4**.*

To a stirred solution of Boc-L-amide (5.5 mmol) in DMF (10 mL), was added Et_3N (12.5 mmol) and HOBt (7.5 mmol). The mixture was allowed to stir for 1 h and then cooled to 0 °C and then EDCI (7.5 mmol) was added. After 1 h, a solution of aniline derivatives (5 mmol) in DMF (10 mL) was added to the above reaction mixture. The resulting mixture was stirred for 7 h at room temperature. After completion as monitored by TLC, the reaction was quenched with ice water and extracted with EtOAc. The organic layer was washed with saturated brine solution, followed by drying over anhydrous Na_2SO_4 and evaporating in vacuo. The crude product was purified by column chromatography (EtOAc / petroleum ether) to give the pure intermediates **2** and **4**.

*4.3.2 General procedure for compounds **6**.*

To a round flask was added **2** or **4** and a standard 50% TFA/CH_2Cl_2 at 0 °C and the stirring was continued for 3 h at room temperature. After completion as monitored by TLC, the reaction was quenched with saturated $NaHCO_3$ solution and extracted with CH_2Cl_2 (3 × 50 mL). The organic layers were dried over anhydrous Na_2SO_4. After removal of the solvent, the crude residue was purified through column chromatography on silica gel (EtOAc/petroleum ether 1: 2 as eluent) to afford compounds **3** and **5**. Compounds **6** were obtained by the condensation of isothiocyanates with **5** in dry CH_2Cl_2 at room temperature for 4 h.

*4.3.3 General procedure for compounds **7**.*

To a stirred solution of compounds **6** (1 mmol) in dry CH_2Cl_2 (10 mL), was added CH_3I (1.5 mmol), K_2CO_3 (1.1mmol) and acetone (5 mL). The mixture was allowed to stir for 30 min at 0°C.Then the sample was stirred at room temperature for 24 h. After the reaction, the solvent was evaporated under reduced pressure, and the crude product was purified by chromatography on silicageleluted with petroleum ether/ethyl acetate (V:V=2:1) to offer compounds **7**.

The structures were confirmed by ^1H NMR, ^{13}C NMR and HR-MS (see supporting information).

4.3.3.1. **N-(1-((3-methoxyphenyl)amino)-1-oxo-3-phenylpropan-2-yl)-3-methyl-2-(3-(3-nitrophenyl)thioureido)pentanamide(6a)**

yellow solid; Yield: 78.8%; ^{1}H NMR (400 MHz, DMSO-d6) δ 10.18 (s, 1H), 9.90 (s, 1H), 8.85 (s, 1H), 8.42 (d, *J* = 8.0 Hz, 1H), 7.97 (d, *J* = 8.2 Hz, 1H), 7.92 (dd, *J* = 8.2, 1.4 Hz, 1H), 7.84 (dd, *J* = 8.1, 1.1 Hz, 1H), 7.58 (t, *J* = 8.2 Hz, 1H), 7.31 (d, *J* = 7.3 Hz, 2H), 7.24 (t, *J* = 7.6 Hz, 3H), 7.21-7.16 (m, 2H), 7.12 (d, *J* = 8.2 Hz, 1H), 6.64 (dd, *J* = 8.1, 1.6 Hz, 1H), 4.89 (t, *J* = 6.7 Hz, 1H, 4.73 (dd, *J* = 13.7, 8.4 Hz, 1H), 3.72 (s, 3H), 3.09 (dd, *J* = 13.9, 5.1 Hz, 1H), 2.96 (dd, *J* = 13.8, 9.4 Hz, 1H), 1.93-1.79 (m, 1H), 1.42(ddd, *J* = 12.1, 7.0, 3.0 Hz, 1H), 1.13-1.03 (m, 1H), 0.83 (dd, *J* = 14.8, 7.3 Hz,6H). ^{13}C NMR (100 MHz, DMSO-d6) δ 180.5, 170.5, 169.7, 159.5, 147.5, 141.0, 139.8, 137.5, 129.7, 129.5, 129.2, 129.2, 128.1, 128.1, 127.9, 126.3, 118.0, 115.9, 111.7, 108.8, 105.3, 61.1, 54.9, 54.9, 37.5, 37.4, 24.4, 15.2, 11.4. HR-MS (m/z) (ESI): calcd for $C_{29}H_{34}N_5O_5S$ [M+H$^+$]: 564.22806; found: 564.22650.

4.3.3.2. **N-(1-((3,4-dimethylphenyl)amino)-1-oxo-3-phenylpropan-2-yl)-3-methyl-2-(3-(3-nitrophenyl)thioureido)pentanamide(6b)**

yellow solid; Yield: 85.70%; ^{1}H NMR (400 MHz, DMSO-d6) δ 10.18 (s, 1H), 9.72 (s, 1H), 8.86 (s, 1H), 8.38 (d, *J* = 8.0 Hz, 1H), 7.97 (d, *J* = 8.2 Hz, 1H), 7.92 (dd, *J* = 8.2, 1.5 Hz, 1H), 7.84 (dd, *J* = 8.1, 1.2 Hz, 1H), 7.58 (t, *J* = 8.2 Hz, 1H), 7.30 (t, *J* = 7.5 Hz, 4H), 7.24 (t, *J* = 7.4 Hz, 2H), 7.16 (t, *J* = 7.2 Hz, 1H), 7.03 (d, *J* = 8.2 Hz, 1H), 4.88 (t, *J* = 6.8 Hz, 1H), 4.72 (dd, *J* = 13.8, 8.5 Hz, 1H), 3.09 (dd, *J* = 13.8, 5.2 Hz, 1H), 2.95 (dd, *J* = 13.7, 9.3 Hz, 1H),2.16 (d, *J* = 5.6 Hz, 6H), 1.91-1.77 (m, 1H), 1.39 (d, *J* = 1.8 Hz, 1H), 1.14-1.02 (m, 1H), 0.83 (dd, *J* = 13.6, 6.8 Hz, 6H). ^{13}C NMR (100 MHz, DMSO-d6) δ 180.4, 170.5, 169.3, 147.5, 141.0, 137.5, 136.4, 136.2, 131.2, 129.7, 129.5, 129.2, 129.2, 128.0, 128.0, 127.8, 126.3, 120.7, 118.0, 117.0, 115.9, 61.2, 54.8, 37.5, 37.4, 24.4, 19.6, 18.7, 15.2, 11.4. HR-MS (m/z) (ESI): calcd for $C_{30}H_{35}N_5O_4S$ [M+Na$^+$]: 584.23074; found: 584.22900.

4.3.3.3. **N-(1-((3-chlorophenyl)amino)-1-oxo-3-phenylpropan-2-yl)-3-methyl-2-(3-(3-nitrophenyl)thioureido)pentanamide(6c)**

yellow solid; Yield: 63.84%; ^{1}H NMR (400 MHz, DMSO-d6) δ 10.17 (s, 1H), 10.13 (s, 1H), 8.84 (s, 1H), 8.47 (d, *J* = 7.7 Hz, 1H), 7.97 (d, *J* = 8.2 Hz, 1H), 7.92 (d, *J* = 8.1 Hz, 1H), 7.84 (d, *J* = 8.1 Hz, 1H), 7.76 (s, 1H), 7.58 (t, *J* = 8.2 Hz, 1H), 7.42 (d, *J* = 8.2 Hz, 1H), 7.32 (dd, *J* = 10.4, 8.1 Hz, 3H), 7.24 (t, *J* = 7.4 Hz, 2H), 7.17 (t, *J* = 7.0 Hz, 1H), 7.11 (d, *J* = 7.9 Hz, 1H), 4.91 (t, *J* = 6.4 Hz, 1H), 4.71 (dd, *J* = 13.8, 7.9 Hz, 1H), 3.09(dd, *J* = 13.8, 5.4 Hz, 1H), 2.97 (dd, *J* = 13.7, 9.2 Hz, 1H), 1.86 (d, *J* = 6.0 Hz, 1H), 1.43(dd, *J* = 8.2, 4.9 Hz, 1H), 1.16-1.02 (m, 1H), 0.84 (dd, *J* =

15.5, 7.3 Hz, 6H). ^{13}C NMR (100 MHz, DMSO-d6) δ 180.4, 170.6, 170.1, 147.5, 141.0, 140.1, 137.3, 133.0, 130.4, 129.7, 129.1, 129.1, 128.1, 128.1, 127.9, 126.4, 123.1, 118.8, 118.0, 117.7, 115.9, 61.0, 55.0, 37.5, 37.3, 24.4, 15.2, 11.4. HR-MS (m/z) (ESI): calcd for $C_{28}H_{31}ClN_5O_4S$ [M+H$^+$]: 568.17853; found: 568.17554.

4.3.3.4. **N-(1-((3-fluorophenyl)amino)-1-oxo-3-phenylpropan-2-yl)-3-methyl-2-(3-(3-nitrophenyl)thioureido)pentanamide(6d)**

yellow solid; Yield: 80%; ^{1}H NMR (400 MHz, DMSO-d6) δ 10.17 (d, *J* = 3.2 Hz, 2H), 8.85 (s, 1H), 8.48 (d, *J* = 7.8 Hz, 1H), 7.97 (d, *J* = 8.2 Hz, 1H), 7.92 (dd, *J* = 8.1, 1.4 Hz, 1H), 7.83 (d, *J* = 8.2 Hz, 1H), 7.61-7.52 (m, 2H), 7.38-7.28 (m, 4H), 7.24 (t, *J* = 7.5 Hz, 2H), 7.18 (d, *J* = 7.2 Hz, 1H), 6.91- 6.82 (m, 1H), 4.94-4.87 (m, 1H), 4.72 (dd, *J* = 13.7, 8.2 Hz, 1H), 3.09(dd, *J* = 13.8, 5.4 Hz, 1H), 2.97 (dd, *J* = 13.7, 9.3 Hz, 1H), 1.90-1.83 (m, 1H), 1.49-1.40(m, 1H), 1.09 (qd, *J* = 14.8, 7.5 Hz, 1H), 0.89-0.78 (m, 6H). ^{13}C NMR (100 MHz, DMSO-d6) δ 180.4, 170.6, 170.1, 163.3, 160.9, 147.5, 141.0, 140.5, 140.4, 137.3, 130.4, 130.3, 129.7, 129.2, 129.2, 128.1, 128.1, 127.9, 126.4, 118.0, 115.9, 115.1, 110.0, 109.8, 106.2, 106.0, 61.0, 54.9, 37.5, 37.3, 26.3, 24.4, 15.2, 11.4. HR-MS (m/z) (ESI): calcd for $C_{28}H_{30}FN_5O_4S$ [M+Na$^+$]: 574.19002; found: 574.18907.

4.3.3.5. **N-(1-((4-methoxyphenyl)amino)-1-oxo-3-phenylpropan-2-yl)-3-methyl-2-(3-(3-nitrophenyl)thioureido)pentanamide(6e)**

yellow solid; Yield: 89.1%; ^{1}H NMR (400 MHz, $CDCl_3$) δ 9.26 (s, 1H), 9.00 (s, 1H*)*, 8.92 (s, 1H), 8.46 (s, 1H), 8.36 (s, 1H), 7.94 (d, *J* = 7.2 Hz, 1H), 7.29 (d, *J* = 8.4 Hz, 2H), 7.22 (s, 2H), 7.18-7.02 (m, 5H), 6.61 (d, *J* = 8.7 Hz, 2H), 5.27 (d, *J* = 23.3 Hz, 2H), 3.67 (s, 3H), 3.20 (s, 2H),1.96 (s, 1H), 1.62(s, 1H), 1.10 (s, 1H), 0.88 (d, *J* = 3.1 Hz, 3H), 0.75 (s, 3H). ^{13}C NMR (100 MHz, $CDCl_3$) δ 180.7, 172.5, 171.0, 157.5, 148.0, 148.0, 140.0, 135.8, 129.9, 129.4, 129.4, 129.0, 128.8, 128.8, 123.7, 123.7, 119.1, 114.2, 114.2, 60.6, 55.4, 55.4, 47.1, 39.3, 25.8, 15.1, 15.1, 11.9, 11.9.HR-MS (m/z) (ESI): calcd for $C_{29}H_{32}N_5O_5S$ [M-H$^+$]: 562.21241; found: 562.21331.

4.3.3.6. **N-(1-((4-bromophenyl)amino)-1-oxo-3-phenylpropan-2-yl)-3-methyl-2-(3-(3-nitrophenyl)thioureido)pentanamide(6f)**

yellow solid; Yield: 82.3%; ^{1}H NMR (500 MHz, DMSO-d6) δ 10.18 (s, 1H), 10.10 (s, 1H), 8.85 (s, 1H), 8.48 (d, *J* = 7.8 Hz, 1H), 7.98 (d, *J* = 8.4 Hz, 1H), 7.92 (dd, *J* = 8.2, 1.6 Hz, 1H), 7.83 (dd, *J* = 8.1, 1.4 Hz, 1H), 7.58 (t, *J* = 8.2 Hz, 1H), 7.55-7.51 (m, 2H), 7.50-7.46 (m, 2H), 7.30 (d, *J* = 7.3 Hz, 2H), 7.24 (t, *J* = 7.5 Hz, 2H), 7.17 (d, *J* = 7.3 Hz, 1H), 4.99-4.78 (m, 1H), 4.70 (d, *J* =

5.5 Hz, 1H), 3.07(dd, *J* = 13.9, 5.4 Hz, 1H), 2.96 (dd, *J* = 13.9, 9.2 Hz, 1H), 1.97-1.72 (m, 1H), 1.57-1.28(m, 1H), 1.12-1.02m, 1H), 0.90-0.75 (m, 6H). ^{13}C NMR (125 MHz, DMSO-d6) δ 180.4, 170.5, 169.9, 147.5, 141.0, 138.1, 137.4, 131.5, 131.5, 129.7, 129.2, 129.2, 128.1, 128.1, 127.8, 126.4, 121.3, 121.3, 118.0, 115.9, 115.0, 61.0, 54.9, 37.5, 37.3, 24.4,15.2, 11.4. HR-MS (m/z) (ESI): calcd for $C_{28}H_{31}BrN_5O_4S$ [M+H$^+$]: 612.12801; found: 612.11157.

4.3.3.7. **N-(1-((4-fluorophenyl)amino)-1-oxo-3-phenylpropan-2-yl)-3-methyl-2-(3-(3-nitrophenyl)thioureido)pentanamide(6g)**

yellow solid; Yield: 86.56%; ^{1}H NMR (500 MHz, DMSO-d6) δ 10.19 (s, 1H), 10.01 (s, 1H), 8.85 (s, 1H), 8.46 (d, *J* = 7.9 Hz, 1H), 7.98 (d, *J* = 8.3 Hz, 1H), 7.92 (dd, *J* = 8.1, 1.4 Hz, 1H), 7.83 (d, *J* = 7.9 Hz, 1H), 7.69-7.52 (m, 3H), 7.31 (d, *J* = 7.3 Hz, 2H), 7.24 (t, *J* = 7.4 Hz, 2H), 7.19-7.07 (m, 3H), 5.18 - 4.82 (m, 1H), 4.71 (dd, *J* = 14.0, 8.3 Hz, 1H), 3.08 (dd, *J* = 13.8, 5.4 Hz, 1H), 2.96 (dd, *J* = 13.7, 9.3 Hz, 1H), 1.86 (d, *J* = 6.2 Hz, 1H), 1.55-1.37(m, 1H), 1.11 (s, 1H), 0.91-0.74 (m, 6H). ^{13}C NMR (125 MHz, DMSO-d6) δ 180.4, 170.5, 169.6, 157.1, 147.5, 141.0, 137.5, 135.1, 129.7, 129.2, 129.2, 128.1, 128.1, 127.9, 126.4, 121.1, 121.1, 118.0, 115.9, 115.4, 115.2, 61.0, 54.9, 37.5, 37.4, 24.4, 15.2, 11.4. HR-MS (m/z) (ESI): calcd for $C_{28}H_{29}FN_5O_4S$ [M-H$^+$]: 550.19243; found: 550.19342.

4.3.3.8. **N-(1-((3,4-dichlorophenyl)amino)-1-oxo-3-phenylpropan-2-yl)-3-methyl-2-(3-(3-nitrophenyl)thioureido)pentanamide(6h)**

yellow solid; Yield: 84.31%; ^{1}H NMR (400 MHz, CD_3OD) δ 8.67 (t, *J* = 2.1 Hz, 1H), 7.96 (ddd, *J* = 8.2, 2.2, 0.9 Hz, 1H), 7.85-7.75 (m, 2H), 7.51 (t, *J* = 8.2 Hz, 1H), 7.36 (d, *J* = 1.3 Hz, 2H), 7.25 (dt, *J* = 14.7, 7.2 Hz, 4H), 7.16 (t, *J* = 7.0 Hz, 1H), 4.79 (dd, *J* = 8.7, 6.4 Hz, 2H), 3.24(dd, *J* = 13.8, 6.4 Hz, 1H), 3.04 (dd, *J* = 13.8, 8.7Hz, 1H), 1.88 (dtd, *J* = 10.1, 6.8, 3.4 Hz, 1H), 1.44 (ddd, *J* = 13.5, 7.6, 3.5 Hz, 1H), 1.16 (ddd, *J* = 13.6, 9.4, 7.3 Hz, 1H), 0.96-0.81 (m, 6H). ^{13}C NMR (100MHz, CD_3OD) δ 183.4, 174.0, 171.8, 149.5, 142.1, 139.2, 138.1, 133.2, 131.4, 130.5, 130.4, 130.4, 129.7, 129.5, 129.5, 128.1, 127.9, 122.9, 120.9, 119.9, 118.5, 63.9, 56.9, 38.7, 38.5, 26.1, 16.0, 11.7. HR-MS (m/z) (ESI): calcd for $C_{28}H_{28}Cl_2N_5O_4S$ [M-H$^+$]: 600.12391; found: 600.12485.

4.3.3.9. **3-methyl-2-(3-(3-nitrophenyl)thioureido)-N-(1-oxo-3-phenyl-1-((3-(trifluoromethyl) phenyl)amino)propan-2-yl)pentanamide(6i)**

yellow solid; Yield: 86.71%; ^{1}H NMR (500 MHz, DMSO-d6) δ 10.31 (s, 1H), 10.19 (s, 1H), 8.85 (s, 1H), 8.53 (d, *J* = 7.7 Hz, 1H), 8.06-7.97 (m, 2H), 7.92 (dd, *J* = 8.2, 1.6 Hz, 1H), 7.84 (dd,

J = 8.1, 1.4 Hz, 1H), 7.77 (d, *J* = 8.0 Hz, 1H), 7.61 - 7.52 (m, 2H), 7.40 (d, *J* = 7.7 Hz, 1H), 7.32 (d, *J* = 7.3 Hz, 2H), 7.25 (t, *J* = 7.5 Hz, 2H), 7.17 (t, *J* = 7.3 Hz, 1H), 4.98-4.88 (m, 1H), 4.72 (dd, *J* = 14.0, 8.2 Hz, 1H), 3.11 (dd, *J* = 13.9, 5.5 Hz, 1H), 2.99 (dd, *J* = 13.9, 9.2 Hz, 1H), 1.87 (dt, *J* = 9.7, 8.1 Hz, 1H), 1.49-1.39(m, 1H), 1.16-0.99 (m, 1H), 0.87 (d, *J* = 6.8 Hz, 3H), 0.83 (t, *J* = 7.4 Hz, 3H). ^{13}C NMR (125 MHz, DMSO-d6) δ 180.4, 170.7, 170.3, 147.5, 141.1, 139.5, 137.4, 130.0, 129.7, 129.2, 129.2, 128.1, 128.1, 127.9, 126.4, 125.2, 122.9, 119.8, 118.0, 115.9, 115.4, 115.4, 61.0, 55.1, 37.6, 37.3, 24.4, 15.2, 11.4. HR-MS (m/z) (ESI): calcd for $C_{29}H_{29}F_3N_5O_4S$ [M-H$^+$]: 600.18923; found: 600.19024.

4.3.3.10. **N-(1-((3-chloro-4-methylphenyl)amino)-1-oxo-3-phenylpropan-2-yl)-3-methyl-2-(3-(3-nitrophenyl)thioureido)pentanamide(6j)**

yellow solid; Yield: 82.5%; ^{1}H NMR (500 MHz, DMSO-d6) δ 10.19 (s, 1H), 10.04 (s, 1H), 8.85 (s, 1H), 8.48 (d, *J* = 7.5 Hz, 1H), 7.99 (d, *J* = 8.0 Hz, 1H), 7.91 (d, *J* = 8.3 Hz, 1H), 7.84 (d, *J* = 7.7 Hz, 1H), 7.75 (s, 1H), 7.58 (t, *J* = 8.1 Hz, 1H), 7.40-7.21 (m, 6H), 7.17 (d, *J* = 7.2 Hz, 1H), 5.00-4.81 (m, 1H, N*CH*), 4.70 (d, *J* = 5.4 Hz, 1H), 3.08 (dd, *J* = 13.7, 5.2 Hz, 1H), 2.96 (dd, *J* = 13.7, 9.3 Hz, 1H), 2.26 (s, 3H), 1.86 (d, *J* = 5.7 Hz, 1H), 1.42 (s, 1H), 1.12-1.03 (m, 1H), 0.90-0.78 (m, 6H). ^{13}C NMR (125 MHz, DMSO-d6) δ 180.4, 170.6, 169.8, 147.5, 141.0, 137.8, 137.4, 133.0, 131.1, 130.1, 129.7, 129.2, 129.2, 128.1, 128.1, 127.8, 126.4, 119.3, 118.0, 115.9, 61.0, 54.9, 37.5, 37.4, 24.4, 18.9, 15.2, 11.4. HR-MS (m/z) (ESI): calcd for $C_{29}H_{31}ClN_5O_4S$ [M-H$^+$]: 580.17853; found: 580.17948.

4.3.3.11. **N-(1-((3-bromophenyl)amino)-1-oxo-3-phenylpropan-2-yl)-3-methyl-2-(3-(4(trifluoromethyl)phenyl)thioureido)pentanamide(6k)**

white solid; Yield: 50.35%; ^{1}H NMR (400 MHz, DMSO-d6) δ 10.12 (s, 2H), 8.46 (d, *J* = 7.7 Hz, 1H), 7.96 (d, *J* = 8.2 Hz, 1H), 7.93-7.81 (m, 3H), 7.65 (d, *J* = 8.6 Hz, 2H), 7.47 (d, *J* = 7.3 Hz, 1H), 7.31 (d, *J* = 7.2 Hz, 2H), 7.25 (td, *J* = 7.8, 2.8 Hz, 4H), 7.18 (d, *J* = 7.2 Hz, 1H), 4.90 (t, *J* = 6.9 Hz, 1H), 4.71 (dd, *J* = 13.9, 8.2 Hz, 1H), 3.09 (dd, *J* = 13.8, 5.5 Hz, 1H), 2.97 (dd, *J* = 13.8, 9.2 Hz, 1H), 1.89-1.79 (m, 1H), 1.42(dtd, *J* = 12.0, 7.7, 4.1 Hz, 1H), 1.09 (dd, *J* = 13.7, 8.9 Hz, 1H), 0.84 (dd, *J* = 14.1, 7.0 Hz, 6H). ^{13}C NMR (100 MHz, DMSO-d6) δ 180.8, 171.1, 170.6, 144.0, 140.8, 137.8, 131.2, 131.2, 129.6, 129.6, 128.6, 128.6, 126.9, 126.5, 126.0, 126.0, 122.2, 122.0, 121.9, 121.9, 118.6, 61.5, 55.4, 38.0, 37.8, 24.9, 15.7, 15.7, 11.9. HR-MS (m/z) (ESI): calcd for $C_{29}H_{31}BrF_3N_4O_2S$ [M+H$^+$]: 635.13032; found: 635.11670.

4.3.3.12. **2-(3-(4-bromophenyl)thioureido)-N-(1-((3-chloro-4-methylphenyl)amino)-1-oxo-3-phenylpropan-2-yl)-3-methylpentanamide(6l)**

white solid; Yield: 55.46%; ^{1}H NMR (400 MHz, DMSO-d6) δ 9.99 (s, 1H), 9.84 (s, 1H), 8.40 (d, *J* = 7.8 Hz, 1H), 7.75 (t, *J* = 5.5 Hz, 2H), 7.56 (d, *J* = 8.7 Hz, 2H), 7.47 (d, *J* = 8.8 Hz, 2H), 7.33 (dd, *J* = 8.3, 1.8 Hz, 1H), 7.29 (d, *J* = 7.2 Hz, 2H), 7.24 (dd, *J* = 12.8, 5.6 Hz, 3H), 7.18 (d, *J* = 7.1 Hz, 1H), 4.87 (s, 1H), 4.68 (d, *J* = 5.8 Hz, 1H), 3.08(dd, *J* = 13.8, 5.5 Hz, 1H), 2.95 (dd, *J* = 13.8, 9.1 Hz, 1H), 2.26 (s, 3H), 1.88-1.72 (m, 1H),1.47-1.35(m, 1H), 1.09-0.97 (m, 1H), 0.86-0.75 (m, 6H). ^{13}C NMR (100MHz, DMSO-d6) δ 180.4, 170.7, 169.8, 139.0, 137.8, 137.4, 132.9, 131.1, 131.1, 131.1, 130.1, 129.1, 129.1, 128.1, 128.1, 126.3, 124.1, 119.3, 118.0, 115.6, 61.1, 54.9, 37.4, 37.3, 24.4, 18.9, 15.2, 15.2, 11.4. HR-MS (m/z) (ESI): calcd for $C_{29}H_{33}BrClN_4O_2S$ [M+H$^+$]: 615.11961; found: 615.10071.

4.3.3.13. **N-(1-((3,4-dichlorophenyl)amino)-1-oxo-3-phenylpropan-2-yl)-3-methyl-2-(3-(3-(trifluoromethyl)phenyl)thioureido)pentanamide(6m)**

white solid; Yield: 70.98%; ^{1}H NMR (400 MHz, DMSO-d6) δ 10.24 (s, 1H), 10.03 (s, 1H), 8.48 (d, *J* = 7.6 Hz, 1H), 8.21 (s, 1H), 7.91 (dd, *J* = 15.0, 5.2 Hz, 2H), 7.71 (d, *J* = 8.2 Hz, 1H), 7.53 (t, *J* = 9.0 Hz, 2H), 7.46 (dd, *J* = 8.8, 2.2 Hz, 1H), 7.41 (d, *J* = 7.6 Hz, 1H), 7.30 (d, *J* = 7.2 Hz, 2H), 7.24 (t, *J* = 7.4 Hz, 2H), 7.16 (t, *J* = 7.1 Hz, 1H), 4.90 (s, 1H), 4.68 (dd, *J* = 14.0, 7.9 Hz, 1H), 3.08 (dd, *J* = 13.8, 5.5 Hz, 1H), 2.97 (dd, *J* = 13.8, 9.1 Hz, 1H), 1.94-1.76 (m, 1H), 1.49-1.37(m, 1H), 1.12 - 1.01 (m, 1H), 0.83 (dd, *J* = 14.5, 7.1 Hz, 6H). ^{13}C NMR (100 MHz, DMSO-d6) δ 180.5, 170.7, 170.2, 140.5, 138.7, 137.2, 130.9, 130.6, 129.5, 129.1, 129.1, 128.1, 128.1, 126.4, 125.6, 124.9, 120.5, 119.3, 61.0, 59.7, 55.0, 37.5, 37.2, 24.4, 20.7, 15.2, 15.2, 14.0, 11.3. HR-MS (m/z) (ESI): calcd for $C_{29}H_{28}F_3Cl_2N_4O_2S$ [M+H$^+$]: 623.12621; found: 623.12512.

4.3.3.14. **3-methyl-N-(1-oxo-3-phenyl-1-((3-(trifluoromethyl)phenyl)amino)propan-2-yl)-2-(3-(3-(trifluoromethyl)phenyl)thioureido)pentanamide(6n)**

white solid; Yield: 38.33%; ^{1}H NMR (400 MHz, $CDCl_3$) δ 9.18 (s, 1H), 8.79 (s, 1H), 8.54 (s, 1H), 7.67 (s, 1H), 7.51 (d, *J* = 12.6 Hz, 2H), 7.42 (d, *J* = 8.2 Hz, 1H), 7.34 (t, *J* = 9.1 Hz, 1H), 7.27 (d, *J* = 7.7 Hz, 1H), 7.24-7.12 (m, 2H), 7.12-7.03 (m, 3H), 6.97 (d, *J* = 6.5 Hz, 3H), 5.06 (s, 2H), 3.22-3.08 (m, 1H), 3.09-2.97 (m, 1H), 1.81 (s, 1H), 1.43 (s, 1H), 0.99 (d, *J* = 6.7 Hz, 1H), 0.76 (d, *J* = 6.3 Hz, 3H), 0.63 (t, *J* = 7.1 Hz, 3H).^{13}C NMR (100 MHz, $CDCl_3$) δ 180.8, 172.3, 170.8, 138.3, 137.5, 135.7, 131.6, 131.3, 129.7, 129.6, 129.3, 129.3, 128.9, 127.7, 127.4, 125.0, 123.7, 122.8,

122.3, 121.8, 121.1, 117.4, 62.9, 56.1, 50.9, 38.5, 38.3, 25.6, 15.2, 11.5. HR-MS (m/z) (ESI): calcd for $C_{30}H_{31}F_6N_4O_2S$ [M+H$^+$]: 625.20719; found: 625.20496.

4.3.3.15. **methyl(Z)-N'-(1-((1-((3,4-dichlorophenyl)amino)-1-oxo-3-phenylpropan-2-yl) amino)-3-methyl-1-oxopentan-2-yl)-N-(3-(trifluoromethyl)phenyl)carbamimidothioate(7a)**

white solid; Yield: 56%; ^{1}H NMR (400 MHz, $CDCl_3$) δ 8.90 (s, 1H), 7.39 (s, 1H), 7.26 (s, 1H), 7.19 (s, 1H), 7.20 - 7.10 (m, 5H), 7.10 - 7.03 (m, 2H), 6.96 (d, *J* = 1.1 Hz, 2H), 6.87 (s, 1H), 6.76 (s, 1H), 4.89 (dd, *J* = 13.8, 6.8 Hz, 1H), 4.24 (s, 1H), 3.08 (d, *J* = 6.5 Hz, 2H), 2.11 (s, 3H), 1.90 (s, 1H), 1.30 (d, *J* = 11.1 Hz, 1H), 1.03 (d, *J* = 6.3 Hz, 1H), 0.83 (d, *J* = 6.7 Hz, 3H), 0.77 (t, *J* = 7.3 Hz, 3H). ^{13}C NMR (100 MHz, $CDCl_3$) δ 172.4, 169.6, 169.6, 136.9, 136.1, 132.4, 131.4, 131.1, 130.2, 129.4, 129.2, 129.2, 128.9, 128.9, 127.6, 127.4, 125.5, 122.8, 121.8, 119.9, 119.4, 119.0, 55.1, 38.0, 25.0, 15.9, 15.9, 14.3, 11.5, 11.5. HR-MS (m/z) (ESI): calcd for $C_{30}H_{32}F_3Cl_2N_4O_2S$ [M+H$^+$]: 639.15751; found: 639.15506.

4.3.3.16. **methyl(Z)-N'-(3-methyl-1-oxo-1-((1-oxo-3-phenyl-1-((3-(trifluoromethyl)phenyl) amino)propan-2-yl)amino)pentan-2-yl)-N-(3-(trifluoromethyl)phenyl)carbamimidothioate(7 b)**

white solid; Yield: 53%; ^{1}H NMR (400 MHz, $CDCl_3$) δ 9.33 (s, 1H), 7.69 (s, 2H), 7.45 (d, *J* = 7.9 Hz, 1H), 7.30-7.10 (m, 10H), 7.02 (s, 1H), 6.91 (s, 1H), 5.14 (d, *J* = 6.6 Hz, 1H), 4.44 (s, 1H), 3.19 (d, *J* = 21.5 Hz, 2H), 2.18 (s, 3H), 2.01 (s, 1H), 1.45 (s, 1H), 1.15 (s, 1H), 0.95 (d, *J* = 6.6 Hz, 3H), 0.86 (t, *J* = 7.3 Hz, 3H). ^{13}C NMR (100 MHz, $CDCl_3$) δ 172.7, 170.0, 170.0, 138.1, 136.2, 129.5, 129.4, 129.3, 129.3, 128.9, 128.9, 127.4, 125.6, 125.3, 123.4, 122.9, 122.6, 121.1, 121.1, 119.7, 119.1, 117.0, 117.0, 55.3, 38.5, 37.2, 27.1, 25.1, 15.9, 14.3, 11.4. HR-MS (m/z) (ESI): calcd for $C_{31}H_{33}F_6N_4O_2S$ [M+H$^+$]: 639.22284; found: 639.22022.

4.3.3.17. **methyl(Z)-N'-(1-((1-((3,4-dimethylphenyl)amino)-1-oxo-3-phenylpropan-2-yl) amino)-3-methyl-1-oxopentan-2-yl)-N-(3-nitrophenyl)carbamimidothioate(7c)**

yellow solid; Yield: 86.96%; ^{1}H NMR (400 MHz, $CDCl_3$) δ 7.98 (s, 1H), 7.87-7.71 (m, 1H), 7.57 (s, 1H), 7.37-7.18 (m, 7H), 7.08 (d, *J* = 7.2 Hz, 1H), 7.03-6.95 (m, 3H), 6.91 (d, *J* = 8.0 Hz, 1H), 5.09 (s, 1H), 4.36 (s, 1H), 3.22 (d, *J* = 6.7 Hz, 1H), 3.16 (dd, *J* = 13.9, 6.9 Hz, 1H), 2.25 (s, 3H), 2.15 (s, 3H), 2.09 (s, 3H), 2.01 (d, *J* = 6.0 Hz, 1H), 1.45 (s, 1H), 1.18-1.07 (m, 1H), 0.93 (d, *J* = 6.8 Hz, 3H), 0.88 (t, *J* = 7.3 Hz, 3H). ^{13}C NMR (100 MHz, $CDCl_3$) δ171.8, 169.0, 169.0, 148.6, 137.0, 136.5, 135.0, 133.0, 129.8, 129.4, 129.4, 128.8, 128.8, 127.2, 121.7, 118.0, 117.6, 117.2,

61.5, 55.0, 53.6, 38.3, 37.0, 31.0, 27.0, 25.1, 19.7, 19.2, 15.8, 14.3, 11.4. HR-MS (m/z) (ESI): calcd for $C_{31}H_{38}N_5O_4S$ [M+H$^+$]: 576.26445; found: 576.26318.

4. 4 Proteasome subunit inhibition assays

The 20S proteasome activity was determined using a Calbiochem proteasome assay kit following the manufacturer's protocol. The chymotrypsin-like activity of the proteasome was assayed by incubating the proteasome (0.5 mg/ml) with the fluorogenic substrate Suc-LLVY-AMC (20 mM) in the presence of proteasome activators and tested compounds. The trypsin-like and caspase-like activities of the 20S proteasome were determined using the fluorogenic substrates Bz-VGR-AMC and (Z)-LLE-bNA, respectively. Cleavage of the substrates by the proteasome resulted in emission of fluorescence, which was measured and expressed as the rate of the reaction by using a Biotek fluorometer. The rate of the cleavage reaction is defined as dF/dt, where dF/dt is the change of fluorescence intensity over time. IC_{50}, calculated by using CalcuSin, is the compound concentration that resulted in 50% decrease in the reaction rate.

4.5 Cytotoxicity assay

The cell lines NCI-H460, HepG2, NCI-H460/DOX, HepG2/DOX and HL-7702 were obtained from the Shanghai Cell Bank in the Chinese Academy of Sciences. NCI-H460, HepG2, NCI-H460/DOX, HepG2/DOX and HL-7702 cell lines were grown on 96-well microtitre plates at a cell density of 10×10^5 cells/well in DMEM medium with 10% FBS. The plates were incubated at 37 ℃ in a humidified atmosphere of 5% CO_2/95% air for overnight. Therewith, the cells were exposed to different concentrations of compounds **3**, **4** and DOX, and incubated for another 48 h. The cells were stained with 10 μl of MTT at incubator for about 4 h. The medium was thrown away and replaced by 100 mL DMSO. The O. D. Value was read at 570/630 nmenzyme labeling instrument.

4.6. Apoptosis analysis

NCI-H460 and NCI-H460/DOX cells were seeded at the density of 2×10^6 cells/mL of the DMEM medium with 10% FBS on 6-well platesto the final volume of 2 mL. The plates were incubated for overnight and then treated with different consentrations compound **6i** for 24 h. Briefly, after treatment with compound **6i** for 24 h, cells were collected and washed with PBS twice, and then resuspend cells in 1×Binding Buffer (0.1 M Hepes/NaOH (pH 7.4), 1.4 M NaCl,

25 mM $CaCl_2$) at a concentration of 1×10^6 cells /ml. The cells were incubated with Annexin V-PE (5 μL) (BD, Pharmingen) and 7-AAD (5 μL) in binding buffer (100 μL) using Annexin V-PE apoptosis kit. Subsequently, the mixture was transfer to a 5 mL culture tube and incubate for 30 min at room temperature. The apoptosis ratio was quantified by system software (CellQuest; BD Biosciences).

4.7 Molecular docking

To study the binding mode of the inhibitors in the active site of 20S proteasome protein, molecular docking was performed using the Surflex-Dock module in SYBYL-X 2.0. The crystal structure of the 20S proteasome complex was retrieved from the RCSB Protein Data Bank (PDB entry code: 3E47) [35]. The ligands were docked in the corresponding protein's binding site by an empirical scoring function and a patented search engine in Surflex-Dock. Before the docking process, the natural ligand was extracted; the water molecules were removed from the crystal structure. Subsequently, the protein was prepared by using the Biopolymer module implemented in Sybyl. The polar hydrogen atoms were added. The automated docking manner was applied in the present work. Other parameters were established by default in the software. Surflex-Dock total scores, which were expressed in $-\log_{10}$ (K_d) units to represent binding affinities, were applied to estimate the ligand-receptor interactions of newly designed molecules.

4. 8 Statistics

The data were processed by the Student' st -test with the significance level $P\leq 0.05$ using SPSS.

Acknowledgements

This study was supported by the National Natural Science Foundation of China (No. 81260472 21362002 and 21431001), Special Research Found for the Doctoral Program of Higher Education (NO. 20134504110002).

References

[1] L. Hong,Y. Piao, Y. Han, J. Wang, X. Zhang, Y. Du, S. Cao, T. Qiao, Z. Chen, D. Fan, Zinc ribbon domain-containing 1 (ZNRD1) mediates multidrug resistance of leukemia cells through regulation of P-glycoprotein and Bcl-2, Mol. Cancer Ther. 4 (2005) 1936-1942.

[2] L. Bedford, J. Lowe, L. R. Dick, R. J. Mayer, J. E. Brownell, Ubiquitin-like protein conjugation and the ubiquitin–proteasome system as drug targets, Nat. Rev. Drug Disc. 10 (2011) 29-46.

[3] H. Ludwig, D. Khayat, G. Giaccone, T. Facon, Proteasome inhibition and its clinical prospects in the treatment of hematologic and solid malignancies, Cancer 104 (2005) 1794-1807.

[4] L. Borissenko, M. Groll, 20S proteasome and its inhibitors: crystallographic knowledge for drug development, Chem. Rev. 107 (2007) 687-717.

[5] S. T. Nawrocki, J. S. Carew, K. Dunner, L. H. Boise, P. J. Chiao, P. Huang, J. L. Abbruzzese, D. J. McConkey, Bortezomib Inhibits PKR-Like Endoplasmic Reticulum (ER) Kinase and Induces Apoptosis via ER Stress in Human Pancreatic Cancer Cells, Cancer Res. 65 (2005) 11510-11519.

[6] P. G. Richardson, C. Mitsiades, T. Hideshima, K. C. Anderson, Bortezomib: proteasome inhibition as an effective anticancer therapy, Annu. Rev. Med. 57 (2006) 33-47.

[7] F. Parlati, S. J. Lee, M. Aujay, E. Suzuki, K. Levitsky, J. B. Lorens, D. R. Micklem, P. Ruurs, C. Sylvain, Y. Lu, K. D. Shenk, M. K. Bennett, Carfilzomib can induce tumor cell death through selective inhibition of the chymotrypsin-like activity of the proteasome, Blood 114 (2009) 3439-3447.

[8] E. Kupperman, E.C. Lee, Y. Cao, B. Bannerman, M. Fitzgerald, A. Berger, J. Yu, Y. Yang, P. Hales, F. Bruzzese, J. Liu, J. Blank, K. Garcia, C. Tsu, L. Dick, P. Fleming, L. Yu, M. Manfredi, M. Rolfe, J. Bolen, Evaluation of the proteasome inhibitor MLN9708 in preclinical models of human cancer, Cancer Res. 70 (2010) 1970-1980.

[9] R. C. Kane, R. Dagher, A. Farrell, C. W. Ko, R. Sridhara, R. Justice, R. Pazdur, Bortezomib for the treatment of mantle cell lymphoma , Clin. Cancer Res. 13 (2007) 5291-5294.

[10] A. Fribley, Q. Zeng, C. Y. Wang, Proteasome Inhibitor PS-341 Induces Apoptosis through Induction of Endoplasmic Reticulum Stress-Reactive Oxygen Species in Head and Neck Squamous Cell Carcinoma Cells, *Mol*e. Cell. Biol. 24 (2004) 9695–9704.

[11] M. Ri, S. Iida, T. Nakashima, H. Miyazaki, F. Mori, A. Ito, A. Inagaki, S. Kusumoto, T. Ishida, H. Komatsu, Y. Shiotsu, R. Ueda, Bortezomib-resistant myeloma cell lines: a role

for mutated PSMB5 in preventing the accumulation of unfolded proteins and fatal ER stress, Leukemia 24 (2010) 1506–1512.

[12] G. Dasmahapatra, D. Lembersky, M. Rahmani, L. Kramer, J. Friedberg, R. I. Fisher, P. Dent, S. Grant, BCL-2 antagonists interact synergistically with bortezomib in DLBCL cells in association with JNK activation and induction of ER stress, Cancer Biol. Ther. 8 (2009) 808-819.

[13] T. Hideshima, C. Mitsiades, M. Akiyama, T. Hayashi, D. Chauhan, P. Richardson, R. Schlossman, K. Podar, N. C. Munshi, N. Mitsiades, K. C. Anderson, Molecular mechanisms mediating antimyeloma activity of proteasome inhibitor PS-341, Blood 101 (2003) 1530–1534.

[14] H. Yamaguchi, K. Bhalla, H. G. Wang, Bax plays a pivotal role in thapsigargin-induced apoptosis of human colon cancer HCT116 cells by controlling Smac/Diablo and Omi/HtrA2 release from mitochondria , Cancer Res. 63 (2003) 1483–1489.

[15] M. Bentires-Alj, V. Barbu, M. Fillet, A. Chariot, B. Relic, N. Jacobs, J. Gielen, M. P. Merville, V. Bours, NFkappaB transcription factor induces drug resistance through MDR1 expression in cancer cells, Oncogene 22 (2003) 90-97.

[16] T. Fujita, K. Washio, D. Takabatake, H. Takahashi, S. Yoshitomi, K. Tsukuda, Y. Ishibe, Y. Ogasawara, H. Doihara, N. Shimizu, Proteasome inhibitors can alter the signaling pathways and attenuate the P-glycoprotein-mediated multidrug resistance, Int. J. Cancer 117 (2005) 670-682.

[17] C. H. Yang, A. Murti, L. M. Pfeffer, Interferon induces NFkappa B-inducing kinase/tumor necrosis factor receptor-associated factor-dependent NFkappa B activation to promote cell survival , J. Biol. Chem. 280 (2005) 31530-31536.

[18] R. Ettari, N. Micale, T. Schirmeister, C. Gelhaus, M. Leippe, E. Nizi, M. E. Di-Francesco, S. Grasso, M. Zappala, Novel peptidomimetics containing a vinyl ester moiety as highly potent and selective falcipain-2 inhibitors, J. Med.Chem. 52 (2009) 2157-2160.

[19] N. Micale, R. Ettari, A. Lavecchia, C. Di Giovanni, K. Scarbaci, V. Troiano, S. Grasso, E. Novellino, T. Schirmeister, M. Zappalà, Development of peptidomimetic boronates as proteasome inhibitors, Eur. J. Med. Chem. 64 (2013) 23-34.

[20] V. Troiano, K. Scarbaci, R. Ettari, N. Micale, C. Cerchia, A. Pinto, T. Schirmeister, E. Novellino, S. Grasso, A. Lavecchia, M. Zappalà, Optimization of peptidomimetic boronates bearing a P3 bicyclic scaffold as proteasome inhibitors, Eur. J. Med. Chem. 83 (2014) 1-14.

[21] R. Ettari, C. Bonaccorso, N. Micale, C. Heindl, T. Schirmeister, M. L. Calabro, S. Grasso, M. Zappal, Development of novel peptidomimetics containing a vinyl sulfone moiety as proteasome inhibitors, Chem. Med. Chem. 6 (2011) 1228-1237.

[22] S. K. Sharma, Y. Wu, N. Steinbergs, M. L. Crowley, A. S. Hanson, R. A. Casero-Jr., P. M. Woster, (Bis)urea and (Bis)thiourea Inhibitors of Lysine-Specific Demethylase 1 as Epigenetic Modulators, J. Med. Chem. 53 (2010) 5197-5212.

[23] X. C. Huang, R. Z. Huang, Z. X. Liao, Y. M. Pan, S. H. Gou, H. S. Wang, Synthesis and pharmacological evaluation of dehydroabietic acid thiourea derivatives containing bisphosphonate moiety as an inducer of apoptosis, Eur. J. Med. Chem. 108 (2016) 381-391.

[24] J. Z. Liu, B. A. Song, H. T. Fan, P. S. Bhadury, W. T. Wan, S. Yang, W. Xu, J. Wu, L. H. Jin, X. Wei, D. Y. Hu, S. Zeng, Synthesis and in vitro study of pseudo-peptide thioureas containing α-aminophosphonate moiety as potential antitumor agents, Eur. J. Med. Chem. 45 (2010) 5108-5112.

[25] C. Alemán, On the ability of modified peptide Links to form hydrogen bonds, J. Phys. Chem. A 105 (2001) 6717–6723.

[26] A. G. Doyle, E. N. Jacobsen, Small-molecule H-bond donors in asymmetric catalysis, Chem. Rev. 107 (2007) 5713–5743.

[27] Jan J. Klein and Stefan Hecht, Synthesis of a New Class of Bis(thiourea)hydrazide Pseudopeptides as Potential Inhibitors of β-Sheet Aggregation, Org. Lett. 14 (2012) 330-333.

[28] P. Liu, C. Li, J. Zhang, X. Xu, Facile and versatile synthesis of alkyl and aryl isothiocyanates by using triphosgene and cosolvent, Synthetic Commum. 43 (2013) 3342–3351.

[29] S. M. Gomha, A facile one-pot synthesis of 6, 7, 8, 9-tetrahydrobenzo [4, 5] thieno [2, 3-d]-1, 2, 4-triazolo [4, 5-a] pyrimidin-5-ones, Monatsh. Chem. 140 (2009) 213–220.

[30] M. Britton, M. M. Lucas, S. L. Downey, M. Screen, A. A. Pletnev, M. Verdoes, R. A. Tokhunts, O. Amir, A. L. Goddard, P. M. Pelphrey, D. L. Wright, H. S. Overkleeft, A. F. Kisselev, Selective inhibitor of proteasome's caspase-like sites sensitizes cells to specific inhibition of chymotrypsin-like sites, Chem. Biol. 16 (2009) 1278-1289.

[31] A. F. Kisselev, A. Callard, A. L. Goldberg, Importance of different active sites in protein breakdown by 26S proteasomes and the efficacy of proteasome inhibitors varies with the protein substrate, J. Biol. Chem. 281 (2006) 8582-8590.

[32] F. Parlati, S. J. Lee, M. Aujay, E. Suzuki, K. Levitsky, J. B. Lorens, D. R. Micklem, P. Ruurs, C. Sylvain, Y. Lu, K. D. Shenk, M. K. Bennet, Carfilzomib can induce tumor cell death through selective inhibition of the chymotrypsin-like activity of the proteasome, Blood 114 (2009) 3439-3447.

[33] E. Szegezdi, S. E. Logue, A. M. Gorman, Mediators of endoplasmic reticulum stress-induced apoptosis, EMBO reports, 7 (2006) 880-885.

[34] B. V. S. Reddy, K. Bhavani, A. Raju, J. S. Yadav, A novel trifunctional organocatalyst for the asymmetric aldol reaction: a facile enantioselective synthesis of β-hydroxyketones, Tetrahedron-Asymm. 22 (2011) 881-886.

[35] M. Groll, O. V. Larionov, R. Huber, A. D. Meijere, Inhibitor-binding mode of homobelactosin C to proteasomes: new insights into class I MHC ligand generation, PNAS 103 (2006) 4576-4579.

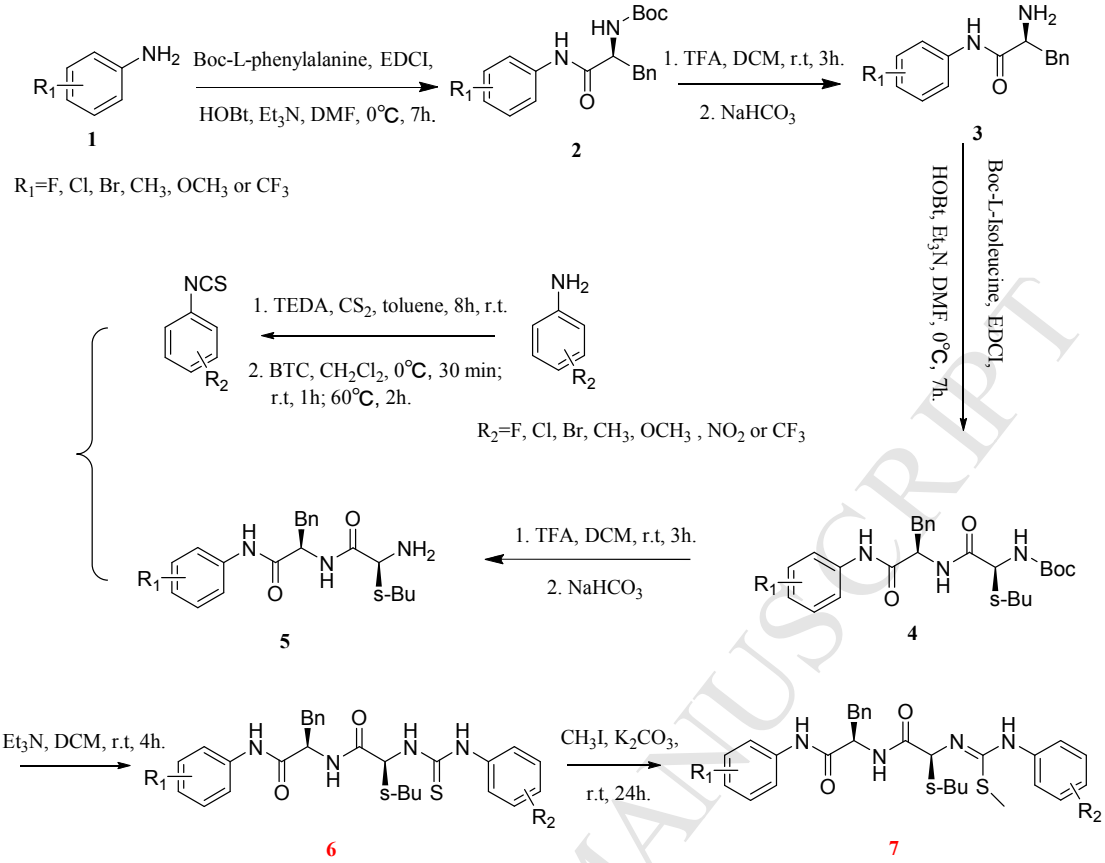

Scheme 1.General synthetic route for compounds **6a-6n** and **7a-7c**.

Tables

Table 1. Inhibition against the ChT-L, T-L and PGPH activity of the human 20S proteasome by tested compounds

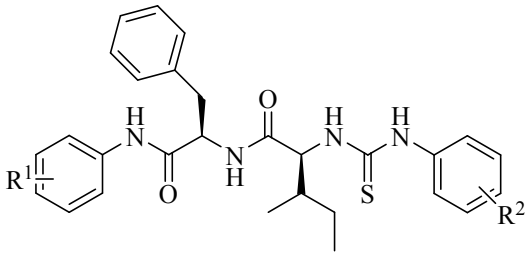

6

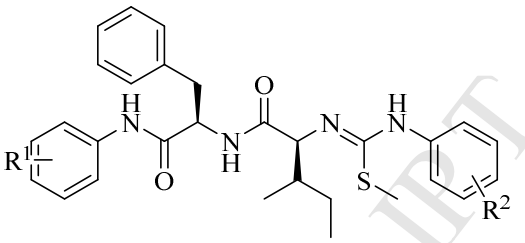

7

Compd.	R^1	R^2	ChT-L(μM)[a]	T-L(μM)[a]	PGPH(μM)[a]
6a	3-CH_3O-phenyl	3- O_2N-phenyl	22.29	n.d.	n.d.
6b	3, 4-CH_3-phenyl	3- O_2N-phenyl	>50	n.d.	n.d.
6c	3-Cl-phenyl	3- O_2N-phenyl	5.84	n.d.	n.d.
6d	3-F-phenyl	3- O_2N-phenyl	3.57	n.d.	n.d.
6e	4-CH_3O-phenyl	3- O_2N-phenyl	29.03	n.d.	n.d.
6f	4-Br-phenyl	3- O_2N-phenyl	2.71	n.d.	n.d.
6g	4-F-phenyl	3- O_2N-phenyl	1.97	n.d.	n.d.
6h	4, 5-Cl-phenyl	3- O_2N-phenyl	1.36	n.d.	n.d.
6i	5-CF_3-phenyl	3- O_2N-phenyl	0.0086	n.i.	34.96
6j	4-CH_3-3-Cl-phenyl	3- O_2N-phenyl	>50	n.d.	n.d.
6k	3-Br-phenyl	4-CF_3-phenyl	0.022	>50	22.74
6l	4-CH_3-3-Cl-phenyl	4-Br-phenyl	>50	n.d.	n.d.
6m	3, 4-Cl-phenyl	3-CF_3-phenyl	0.017	n.i.	15.14
6n	3-CF_3-phenyl	5-CF_3-phenyl	19.60	n.d.	n.d.
7a	3,4-Cl	5-CF_3	22.16	n.d.	n.d.
7b	5-CF_3	5-CF_3	8.83	n.i.	22.63
7c	3, 4-CH_3	3- O_2N	>50	n.d.	n.d.
MG-132	-	-	0.025	n.d.	n.d.

[a] The IC_{50} values are for inhibition against the ChT-L, T-L and PGPH activity of the human 20S proteasome.

n.d. = not determined;

n.i. = no inhitition.

Table 2 Docking scores (kcal/mol) for all studied compounds

Comd.	Total score	Crash	Polar	G_score	PMF_score	D-score	Chem score	Cscore
6a	7.74	-1.11	0.00	-129.58	29.58	-291.52	-17.47	2
6b	6.61	-1.57	1.99	-143.54	35.50	-247.27	-23.68	3
6c	8.68	-0.85	2.17	-139.80	8.33	-238.33	-21.33	2
6d	8.76	-2.07	0.76	-135.41	42.51	-288.33	-20.11	2
6e	7.53	-1.78	2.29	-166.21	7.31	-306.72	-31.07	4

6f	9.02	-2.26	1.01	-166.56	20.40	-331.18	-25.94	4
6g	9.24	-0.54	3.00	-123.18	-8.18	-207.05	-24.44	3
6h	9.43	-1.45	0.51	-123.05	16.43	-242.50	-15.65	2
6i	12.63	-2.97	0.88	-157.34	4.35	-331.93	-24.42	4
6j	6.11	-1.07	1.29	-133.50	18.81	-244.21	-23.99	5
6k	10.23	-1.46	1.56	-173.49	37.24	-309.90	-27.48	4
6l	7.00	-2.33	0.05	-141.51	24.68	-285.44	-21.77	2
6m	11.51	-2.50	0.71	-155.14	25.55	-327.30	-25.99	4
6n	8.59	-3.16	0.96	-126.263	22.35	-269.87	-24.67	4
7a	8.12	-1.18	0.73	-135.19	10.58	-102.58	-21.65	2
7b	9.50	-2.25	0.01	-164.39	36.52	-220.20	-23.12	4
7c	6.97	-1.74	0.08	-177.84	44.11	-190.03	-24.91	3
3E47-ligand	8.73	-1.18	0.99	184.17	57.97	-297.49	-19.19	4
MG-132	9.22	-2.51	2.44	-169.76	21.49	-304.84	-28.17	4

Table 3. Cytotoxic effects of tested compound**s** on NCI-H460/DOX and HepG2/DOX Cell Lines

Compd.	IC_{50} (μM)[a]						
	NCI-H460	NCI-H460/DOX	resistant factor	HepG2	HepG2/DOX	resistant factor	HL-7702
6c	13.64±1.73	31.67±1.04	2.32	20.72±1.32	>50	-	>50
6d	12.26±0.48	28.56±1.10	2.33	18.02±0.99	36.76±1.03	2.04	>50
6f	16.16±1.14	35.19±0.81	2.18	17.45±1.14	48.21±0.53	2.76	>50
6g	20.23±1.02	42.35±1.50	2.09	17.52±1.50	48.49±0.95	2.78	>50
6h	14.83±1.09	32.33±0.94	2.18	13.26±0.70	37.41±1.16	2.82	>50
6i	1.70±1.16	6.74±1.87	3.96	4.80±1.23	10.18±1.53	2.12	>50
6k	**7.13±1.44**	11.24±1.33	1.58	**18.62±1.32**	27.43±0.79	1.47	>50
6m	**6.14±1.34**	15.51±1.02	2.52	**12.12±1.12**	29.61±1.68	2.44	>50
7b	20.29±0.95	>50	-	19.31±1.54	49.18±1.13	2.55	>50
DOX	5.18±1.75	>50	-	6.91±0.96	>50	-	12.23±1.24

Figures captions

Fig. 1 Chemical structures of 20S proteasome inhibitors.

Fig. 2 Binding mode of compound **6i** (a), ligand (b) and MG132 (c) in the active site of 3E47, respectively. Ligands and the important residues for binding interactions are represented by stick and line models. The hydrogen bonds are shown as yellow dotted lines (color figure online).

Fig. 3 Apoptotic effects of compound **6i**. NCI-H460 cells (A-C) and NCI-H460/DOX cells (D-F) were treated with compound **6i** or LY335979 at the indicated concentrations for 24 h. The apoptotic effects were analyzed by flow cytometry.

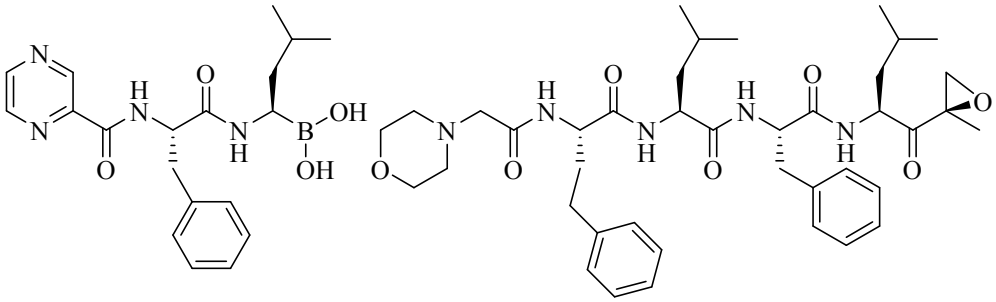

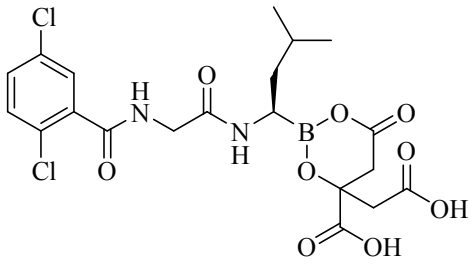

Fig. 1 Chemical structures of 20S proteasome inhibitors.

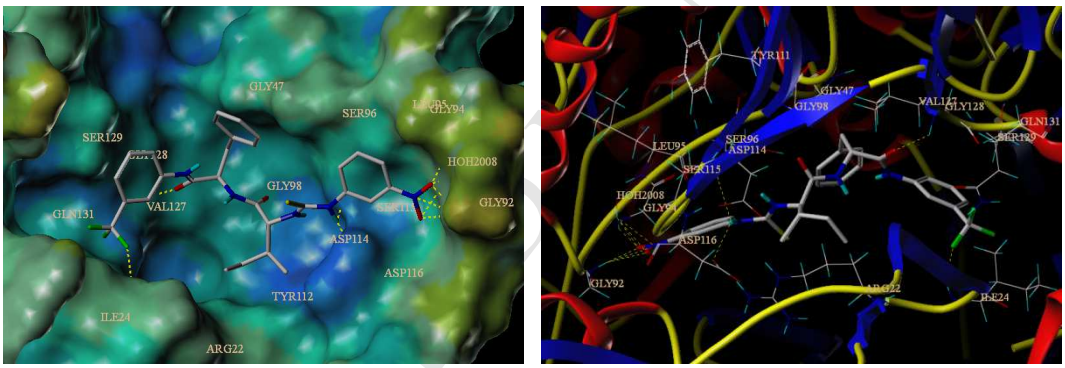

6i (a)

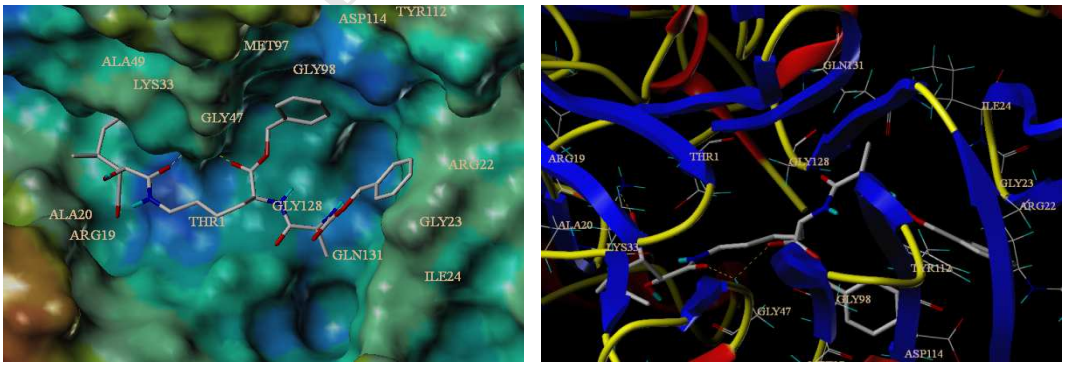

3E47-ligand (b)

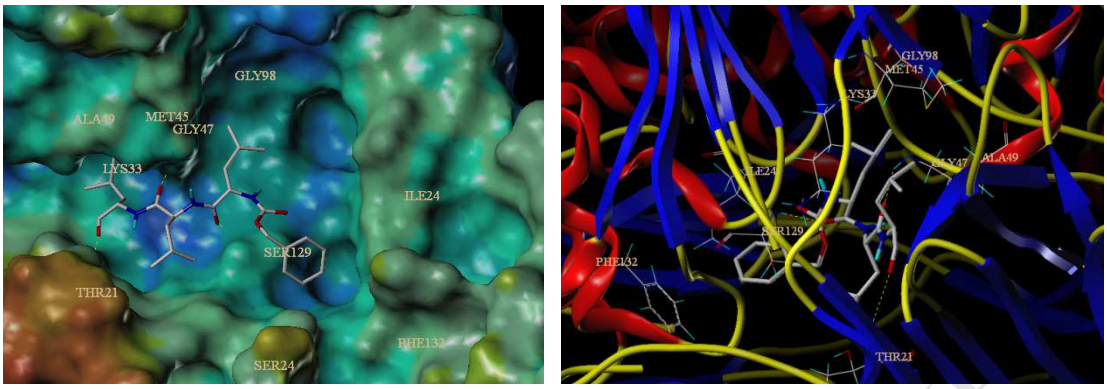

MG-132 (c)

Fig. 2 Binding mode of compound **6i** (a), ligand (b) and MG132 (c) in the active site of 3E47, respectively. Ligands and the important residues for binding interactions are represented by stick and line models. The hydrogen bonds are shown as yellow dotted lines (color figure online).

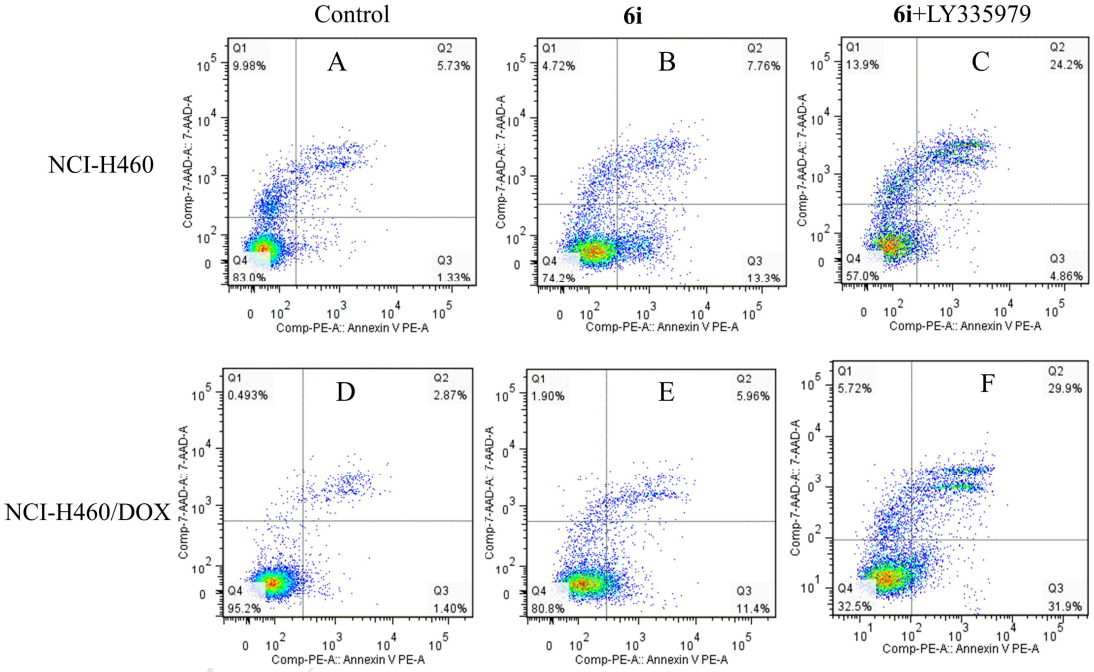

Fig. 3 Apoptotic effects of compound **6i**. NCI-H460 cells (A-C) and NCI-H460/DOX cells (D-F) were treated with compound **6i** or LY335979 at the indicated concentrations for 24 h. The apoptotic effects were analyzed by flow cytometry.

Highlights

- A novel series of the terminal functionalized dipeptides derivatives containing thiourea group moiety were synthesized.
- Compound **6i** exhibited remarkable ChT-L proteasome inhibitory activity.
- Molecular modeling suggested that **6i** tightly binds to the active site of 20S proteasome.
- The inhibitors efficiently block survival of doxorubicin-resistant human lung cancer cells.
- **6i** induced apoptosis in NCI-H460 and NCI-H460/DOX cells.